

PS **Turbidity Current Flows over Rough Substrates***

Armin Arfaie¹, Alan D. Burns^{1,2}, Derek B. Ingham^{1,2}, Joris T. Eggenhuisen^{1,4}, Robert M. Dorrell^{1,3}, and William D. McCaffrey^{1,3}

Search and Discovery Article #41426 (2014)**

Posted August 29, 2014

*Adapted from poster presentation given at 2014 AAPG Annual Convention and Exhibition, Houston, Texas, April 6-9, 2014

**AAPG © 2014 Serial rights given by author. For all other rights contact author directly.

¹Turbidites Research Group, University of Leeds, UK (pm10aa@leeds.ac.uk)

²Energy Technology and Innovation Initiative (ETII), University of Leeds, UK

³School of Earth and Environmental, University of Leeds, UK

⁴Utrecht University, The Netherlands

Abstract

Although many turbidity currents propagate over lower boundaries characterized by form roughness, there have been few experimental and numerical investigations of turbidity current flow over dynamically rough substrates. This research aims to investigate the influence of roughness height and spacing on sediment entrainment potential, erosion and rate of sedimentation (deposition). Specific questions include: (i) do lower boundary interactions in the hydraulically smooth vs. rough cases cause differential turbidity current propagation?, (ii) is any coupling between the flow and substrate one-way or two way?, (iii) in the latter case, what are the implications for linked flow and substrate evolution?

Accordingly, a numerical study of flow over rough substrates has been undertaken for a wide range of roughness spacings and Reynolds number. LES and DNS numerical modeling of such a wide range of roughness spacings is problematic due to the computational resources, the number of cases and the Reynolds number range. Therefore, a RANS (Reynolds Averaged Navier-Stokes) based turbulence modeling approach is adopted using a commercial CFD code, ANSYS-CFX 14.5. The modeled scenario is a channel with lower boundary roughness comprising square bars on the bottom wall, oriented transverse to the flow direction. Initial results suggest turbulence maxima occur when the ratio of object spacing to object width (the pitch ratio) is ~ 7 .

This value is only weakly dependent on Reynolds number. The decay rate of turbulence enhancement beyond this optimum spacing is rather low. Further work has examined the influence of the obstacles height on the peak turbulence enhancement of the flow below the boundary layer, across a range of pitch ratios and Reynolds number conditions. The implications of likely lower boundary roughness effects for prediction of flow depletion and run-out distance are investigated.

Armin Arfaie^{1,2}, Alan D. Burns^{1,2}, Derek B. Ingham^{1,2}, Joris T. Eggenhuisen^{1,4}, Robert M. Dorrell^{1,3} and William D. McCaffrey^{1,3}

¹ Turbidites Research Group, University of Leeds (UK), ² Energy Technology and Innovation Initiative (ETII), University of Leeds (UK), ³ School of Earth and Environmental, University of Leeds (UK), ⁴ Utrecht University (the Netherlands), *Corresponding author. Email address: pm10aa@leeds.ac.uk

Introduction

- Although Many turbidity currents propagate over lower boundaries characterized by form roughness, there have been few experimental and numerical investigations of turbidity current flow over dynamically rough substrates. The rough substrates form either through erosion to leave a rugose lower boundary, or via the construction of aggradational bed forms.
- The surface roughness of the deep-sea floor plays an important role in the turbulence structure of turbidity currents (Meiburg and Kneller, 2010; Macdonald et al., 2011; Eggenhuisen and McCaffrey, 2012).
- Shear flows have major effects on the flow transportation dynamics of turbidity currents. Previous studies suggest an apparent similarity in the inner and outer layer of the turbidity current respectively to the viscous and inviscid layers of a plane half-channel turbulent shear flow. Such similarities provide incentives for studying rough channel shear flow in tackling turbidity currents fluid dynamics problems. Thus, measurements of turbulence quantities such as friction factor and eddy viscosity of plane turbulent wall jets can provide initial insight on implications for natural turbidity currents.
- Accordingly, a numerical study of flow over rough substrates has been undertaken for a wide range of roughness spacings and Reynolds number. The modeled scenario is a channel with lower boundary roughness comprising square bars on the bottom wall, oriented transverse to the flow direction.



Figure 3: Image of flute casts in Catagnola system.

Objectives

- This research aims to investigate the influence of roughness height and spacing on sediment entrainment potential, erosion and rate of sedimentation (deposition). Specific questions include:

(i) How do flow interactions with lower boundary roughness elements affect the dynamical structure of the flow?

(ii) What is the optimum spacing of the roughness elements that would maximise the turbulence within the flow? Do lower boundary interactions in the hydraulically smooth vs. fully rough cases cause differential turbidity current propagation?

(iii) Is any coupling between the flow and substrate one-way or two way? In the latter case, what are the implications for linked flow and substrate evolution?

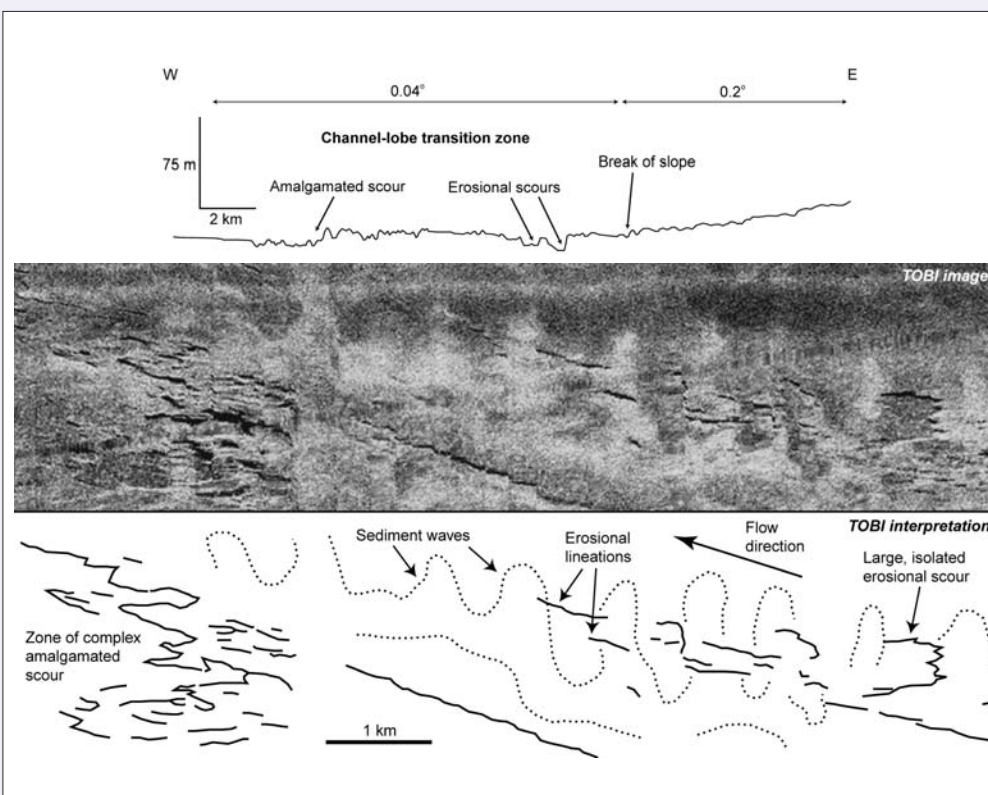


Figure 1: Sketch of the TOBI profile and interpretation indicating erosional and sediment waves in the proximal Agadir CLTZ (from Wynn et al., 2002).

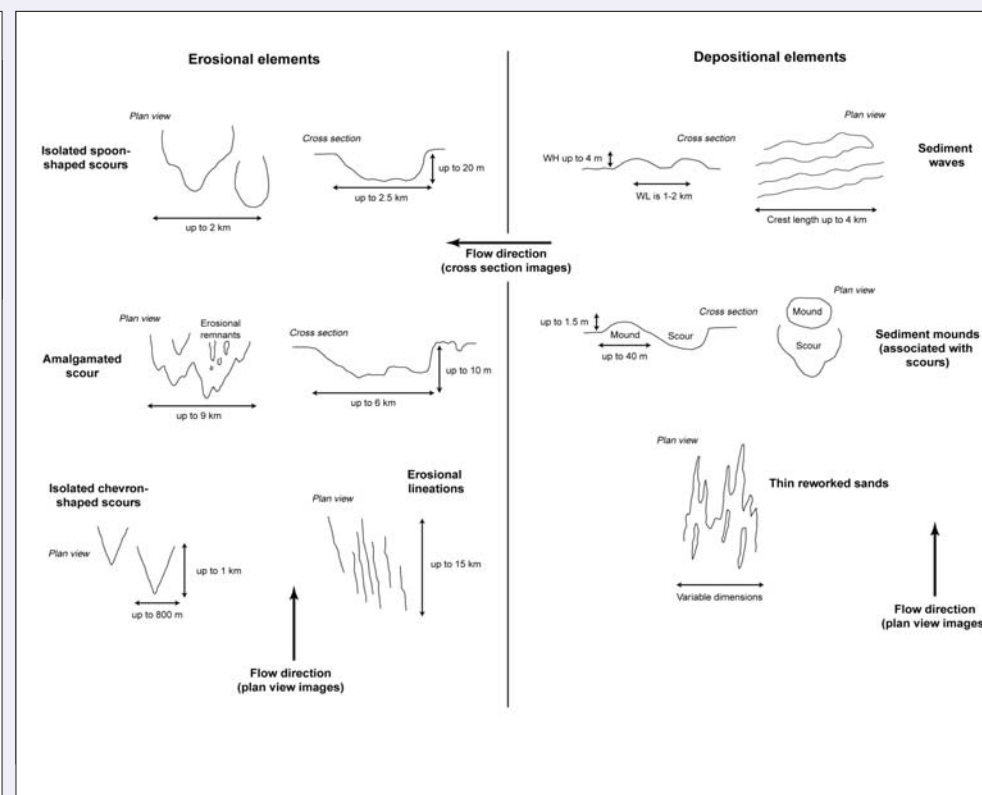


Figure 2: The typical morphology and dimensions of erosional and depositional features within CLTZ (from Wynn et al., 2002).

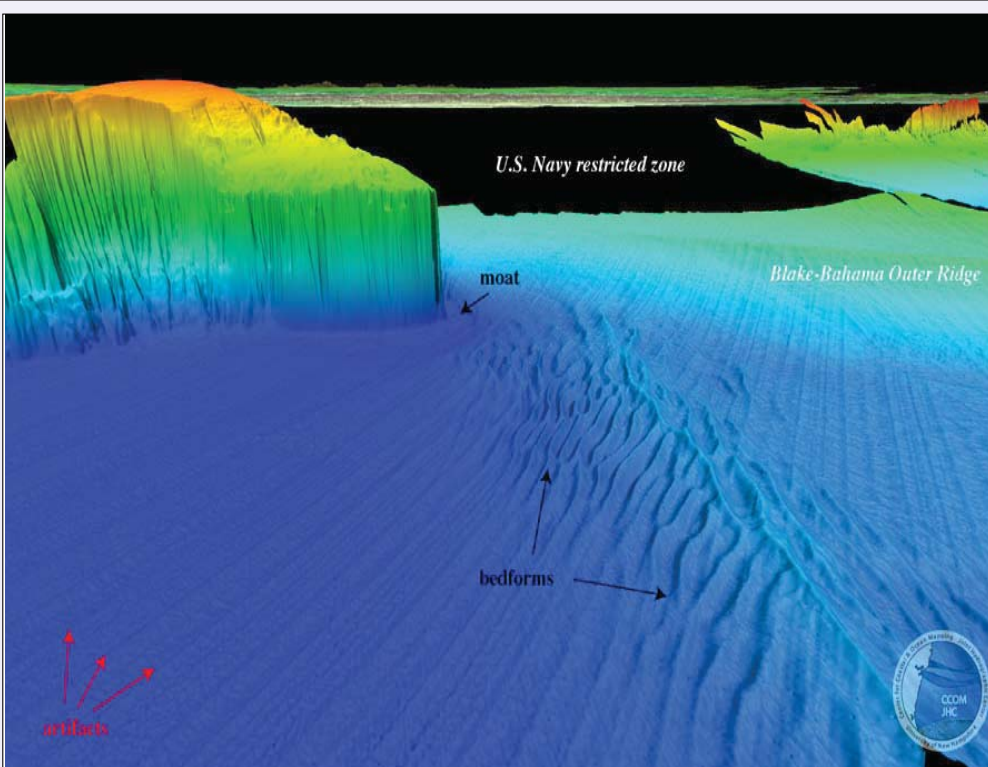


Figure 4: Perspective view of the bathymetry of Blake Spur showing bedforms in a linear trend (Images taken from CCOM/JHC, The University of New Hampshire, Durham, USA).

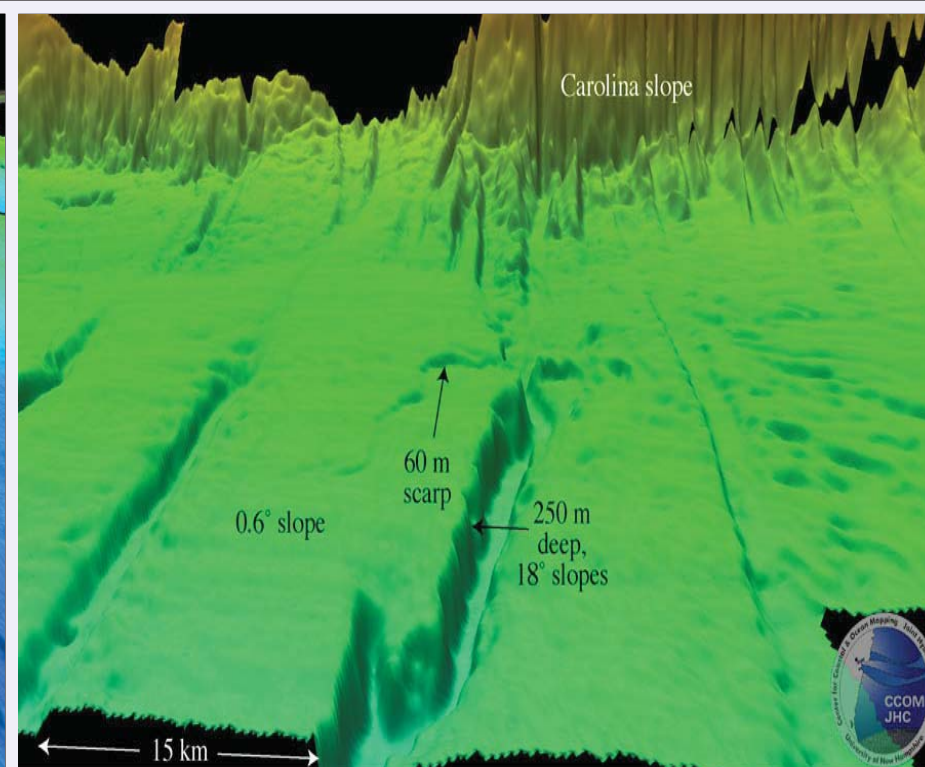


Figure 5: Perspective view of the bathymetry in the Carolina margin showing the pattern and dimensions of large-scaled bedforms (Image taken from CCOM/JHC, The University of New Hampshire, Durham, USA).

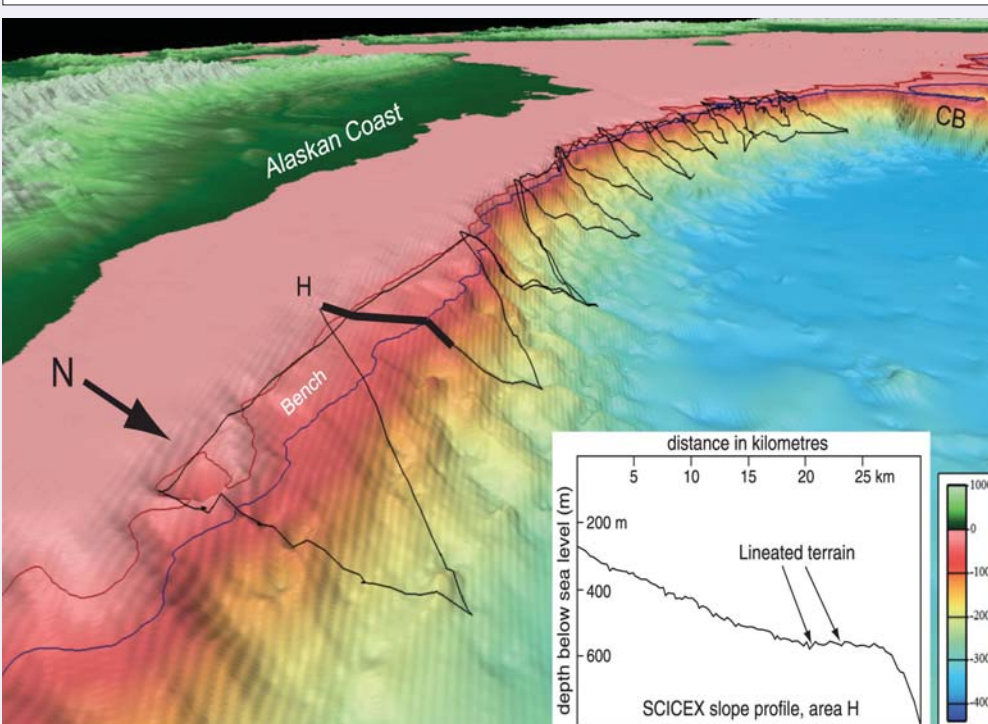


Figure 6: The view of the Alaska Beaufort margin showing the slope-parallel lineated train on the bathymetric bench along margin in Area H (from Engels et al., 2008).

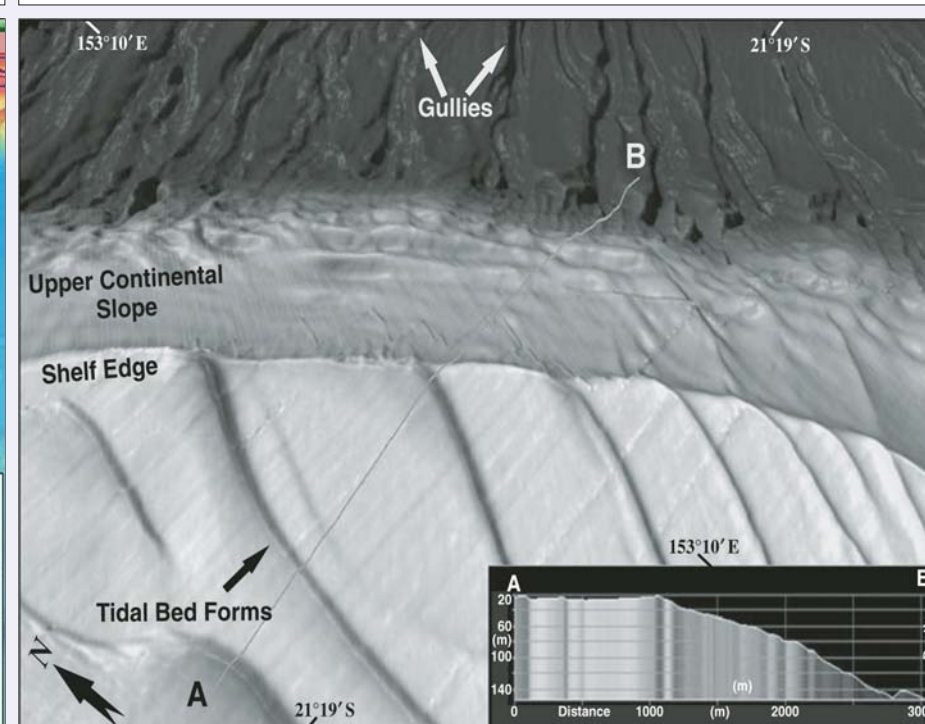


Figure 7: Tidal bed forms directing eastward out of Hervey Bay in southeast Australia across continental shelf and over shelf edge (from Boyd et al., 2014).

Numerical Method

- Steady state Computational Fluid Dynamics (CFD) simulations have been performed using the commercial code, ANSYS CFX 14.0. This code uses a finite volume method to solve the Reynold time averaged Navier-Stokes (RANS) equations by a coupled solver.

- Numerous turbulence models were employed for comparisons against experimental and numerical results in literature.

- The mathematical equations for steady Reynolds averaged models are based on conservation of fluid mass, continuity and momentum as follows:

Continuity:

$$\frac{\partial \bar{U}_i}{\partial x_i} = 0$$

Momentum:

$$\frac{\partial}{\partial x_j} (\rho \bar{U}_i \bar{U}_j) = -\frac{\partial \bar{p}}{\partial x_i} + \frac{\partial}{\partial x_j} \left[\mu_{eff} \left(\frac{\partial \bar{U}_i}{\partial x_j} + \frac{\partial \bar{U}_j}{\partial x_i} \right) \right] + S_M$$

$$\bar{p} = \bar{p} + \frac{2}{3} \rho K + \frac{2}{3} \mu_{eff} \frac{\partial U_k}{\partial x_k}$$

The effective viscosity:

$$\mu_{eff} = \mu + \mu_t$$

The turbulent viscosity:

$$\mu_t = C_\mu \rho \frac{K^2}{\epsilon}$$

Armin Arfaie^{1,2}, Alan D. Burns^{1,2}, Derek B. Ingham^{1,2}, Joris T. Eggenhuisen^{1,4}, Robert M. Dorrell^{1,3} and William D. McCaffrey^{1,3}

¹ Turbidities Research Group, University of Leeds (UK), ² Energy Technology and Innovation Initiative (ETII), University of Leeds (UK), ³ School of Earth and Environmental, University of Leeds (UK), ⁴ Utrecht University (the Netherlands), *Corresponding author. Email address: pm10aa@leeds.ac.uk

Flow Configuration

- Figure 8 displays the computational domain with its co-ordinate system and the roughness element shape.
- The roughness element is in a non-staggered, two-dimensional transverse square arrangement, with a cross section $k \times k$, positioned on the lower boundary.
- Periodic boundary conditions are used in the streamwise direction and a symmetry condition is applied in the spanwise direction. A no-slip boundary condition was applied to the upper and lower wall. A mean pressure gradient is imposed as a source term in the U-momentum equation.
- The width-to-height ratio w/k was varied from 0.12 to 402.
- The roughness element height is $0.05H$, where H is the full channel height.
- The simulations have been performed for 28 domains for a range of dp/dx (mean pressure gradient) values.
- Figure 9 shows the computational domain for case study B. In this case, the roughness element to channel height ratio, h/H is varied.
- The Shear Reynolds number Re_τ , and the bulk Reynolds number Re_b , respectively are determined as follows:

$$Re_\tau = (H/2) u_\tau / \nu$$

$$Re_b = (H/2) U_b / \nu$$

H is the full channel height

Case Study A: Variation in roughness elements spacing

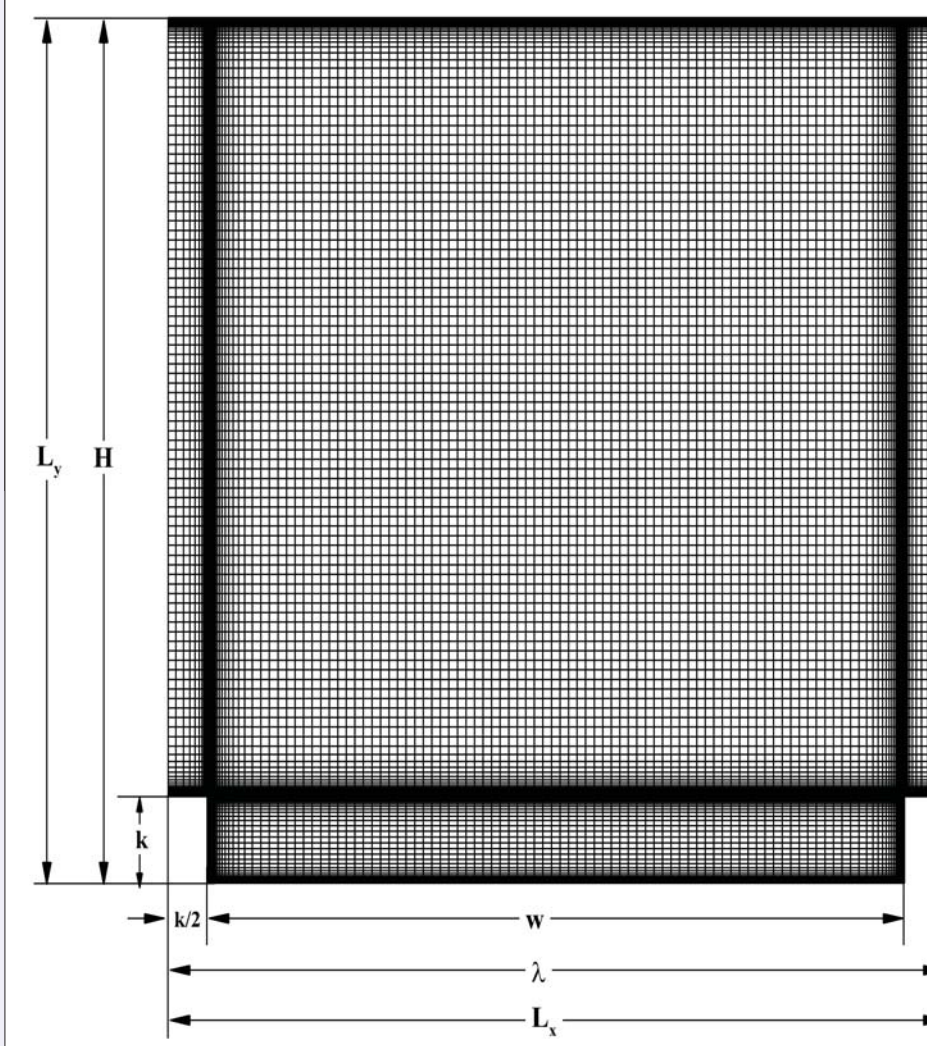


Figure 8: Computational domain and hexahedral grid system of the channel flow with surface roughness showing the parameters for $w/k=9$.

Case Study B: Variation in roughness elements heights

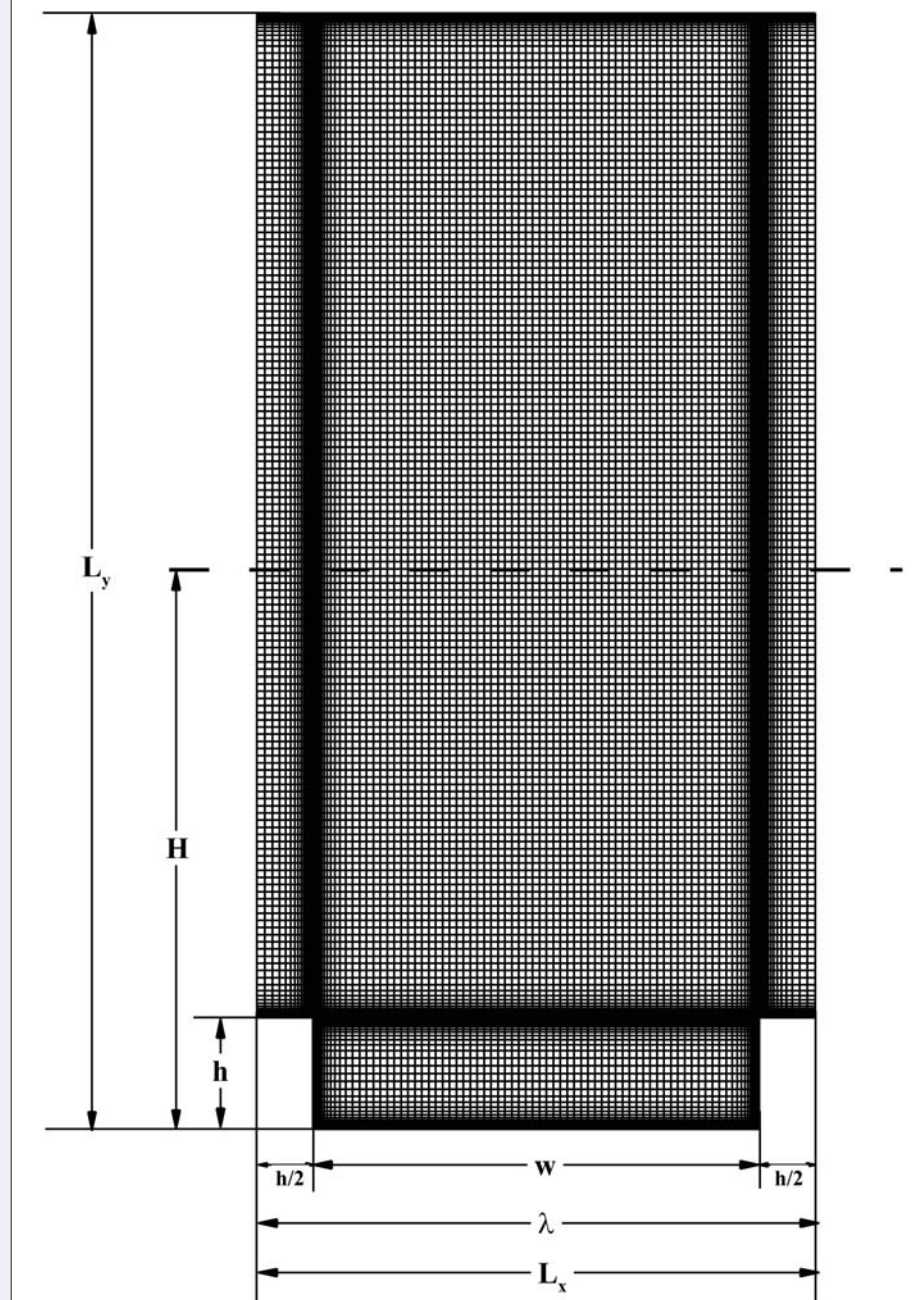


Figure 9: Geometry and computational grid for the channel flow with rib roughness on the lower boundary.

Model Validation

- The Figures 9 (a)-(d) show the streamwise velocity profiles normalised by the maximum streamwise velocity obtained from the turbulence model solutions for $w/k=1, 4, 8, 9$. The velocity profiles are displayed for a line located at the centre of the channel in the cavity from the upper to the lower wall boundaries.
- Overall for all the turbulence models, the velocity profiles show a reasonable agreement with previous numerical and experimental data. The K- ϵ model shows best agreement with available data. The normalised turbulence intensity results are more sensitive and show discrepancies. As illustrated in figure 9 (e)-(f), RANS models show poor prediction of the turbulence intensities.
- Figure 10 shows the wall pressure drag distribution along a line positioned at the bottom of the cavity for $w/k=9$. This distance is normalised by the roughness height k , and K- ϵ model is tested for validation. The agreement between the RANS computation and LES is satisfactory.
- The K- ϵ turbulence model demonstrates a reasonable prediction in capturing velocity profiles. Therefore, the predictions of the eddy viscosity must be reasonably accurate, as the influence of turbulence on the flow field is largely governed by the eddy viscosity term. Moreover, turbulent dispersion of heat and small particles may be modelled using an eddy diffusivity which is proportional to the eddy viscosity. Therefore, K- ϵ turbulence model has been used to further examine the characteristics of the roughened wall flow over a range of aspect ratios.

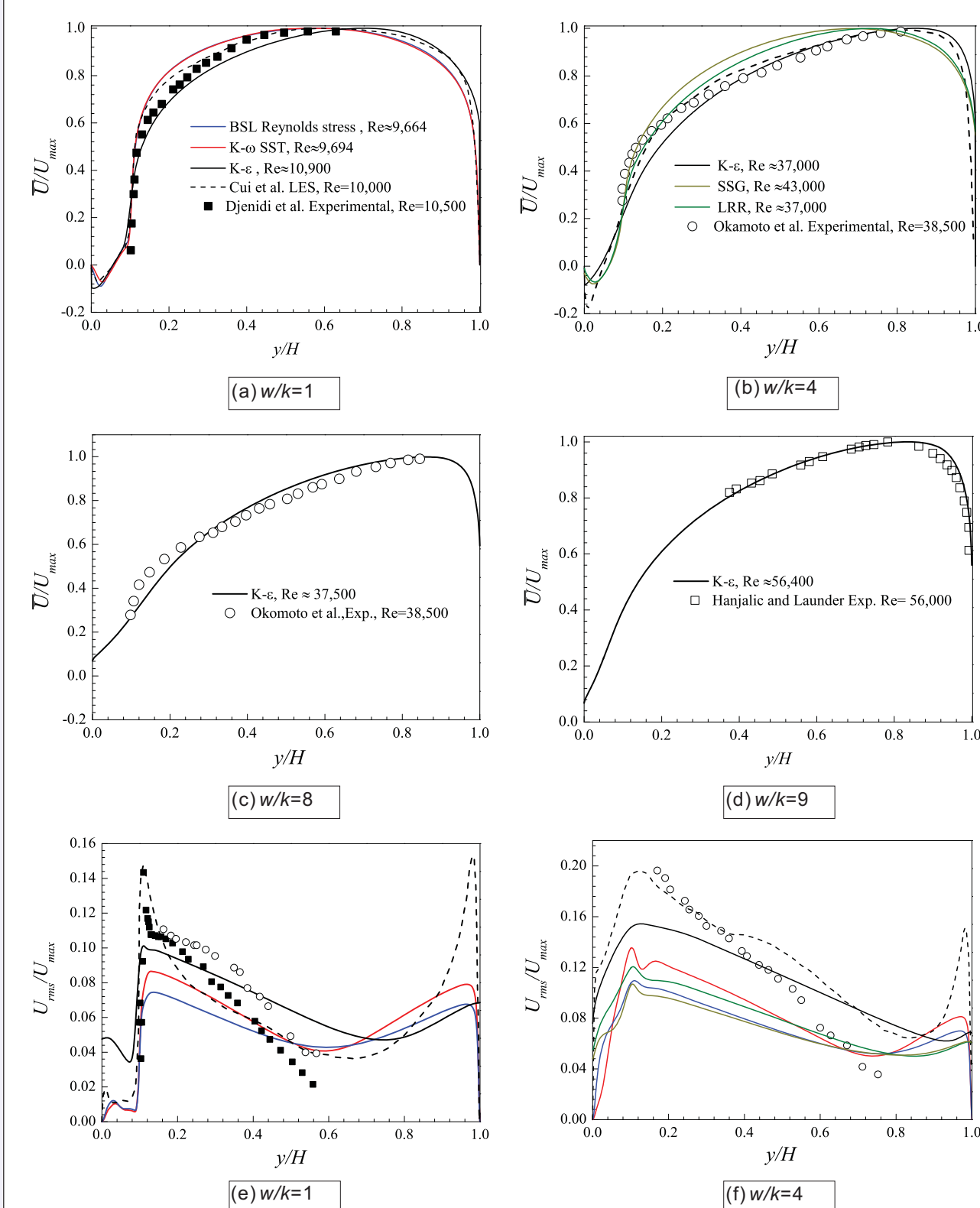


Figure 9: Plots of the computed velocity profiles of various turbulence models on the centre line of the channel for (a) $w/k=1$, (b) $w/k=4$, (c) $w/k=8$ at $Re \approx 56,000$ (d) $w/k=9$ at $Re \approx 37,000$ and (e) turbulence intensity at $w/k=1$ (f) turbulence intensity at $w/k=4$, with the experimental and numerical (LES) results.

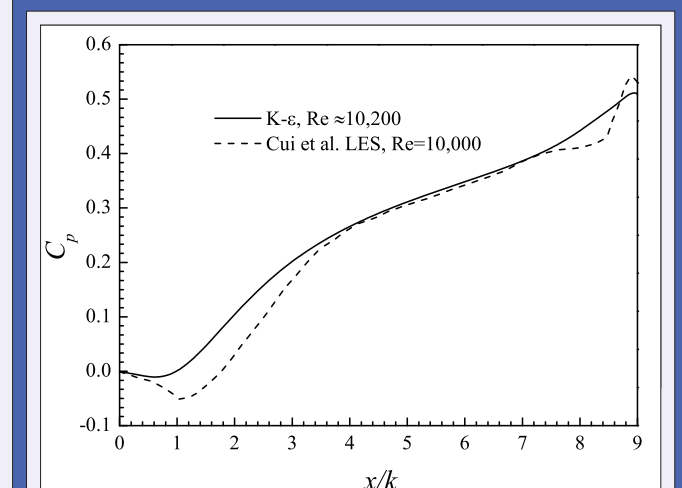


Figure 10: The pressure coefficient profile at $w/k=9$.

Armin Arfaie^{1,2}, Alan D. Burns^{1,2}, Derek B. Ingham^{1,2}, Joris T. Eggenhuisen^{1,4}, Robert M. Dorrell^{1,3} and William D. McCaffrey^{1,3}

¹ Turbidites Research Group, University of Leeds (UK), ² Energy Technology and Innovation Initiative (ETII), University of Leeds (UK), ³ School of Earth and Environmental, University of Leeds (UK), ⁴ Utrecht University (the Netherlands), *Corresponding author. Email address: pm10aa@leeds.ac.uk

Results

Modelling simulations were performed to study turbulent flow over two-dimensional square roughness elements for various Reynolds numbers and w/k ratios (Case study A). The streamlines and reattachment length of the averaged two-dimensional velocity field of the results are presented. The flow is over form-type roughness. Thus, the viscous effect of the wall will be negligible relative to the pressure drag produced by the rib. Finally, to further characterise the bed roughness, flow resistance and eddy viscosity variation are evaluated. The dependence of these results on the Reynolds number as a function of width-to-height ratio will be discussed.

More simulations have been performed to investigate the effect of roughness to channel height ratio, h/H on the optimal mixing and the flow resistance (Case study B).

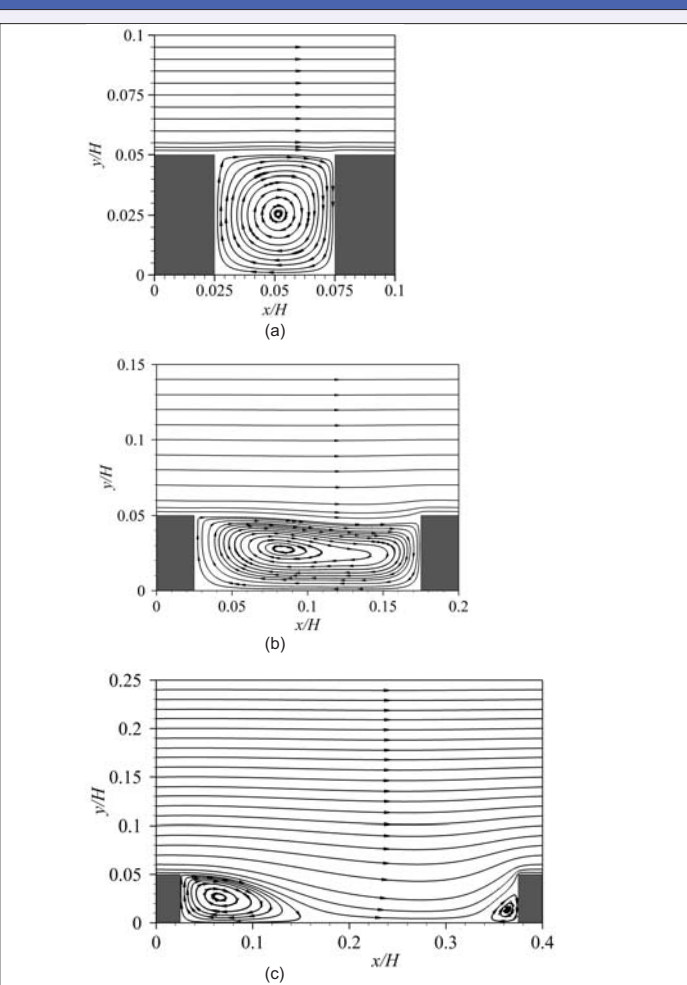


Figure 11: Distribution of mean streamlines velocity for (a) $w/k=1$, (b) $w/k=3$, (c) $w/k=7$.

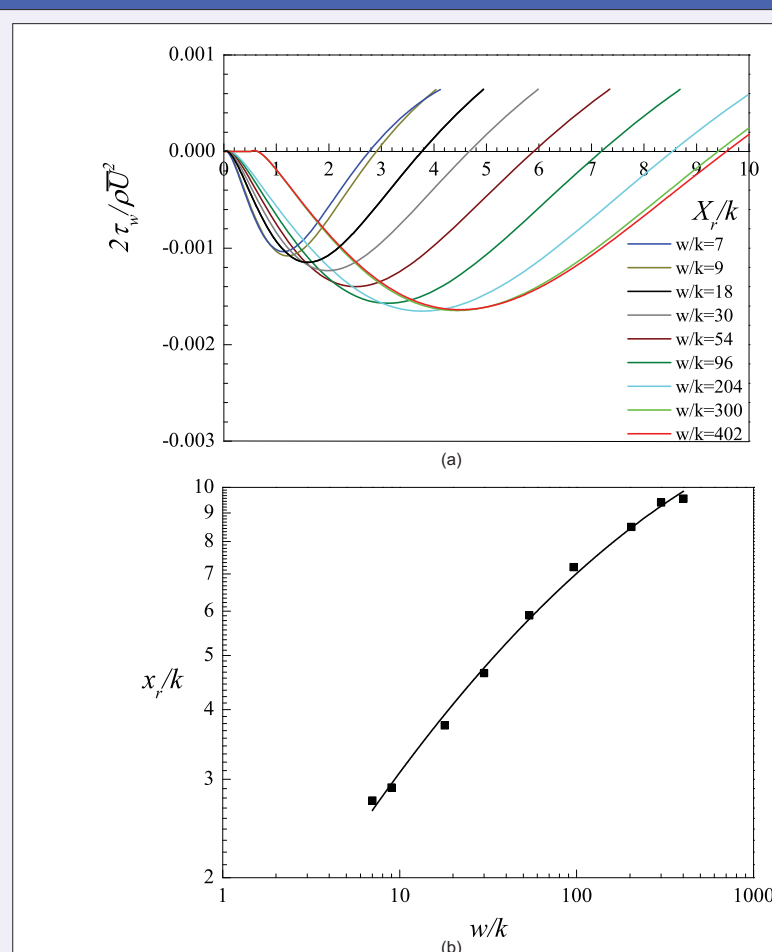


Figure 12: (a) The normalised wall shear stress versus the normalised distance between the adjoining ribs and (b) Graph of the reattachment point with varying the width-to-height ratio.

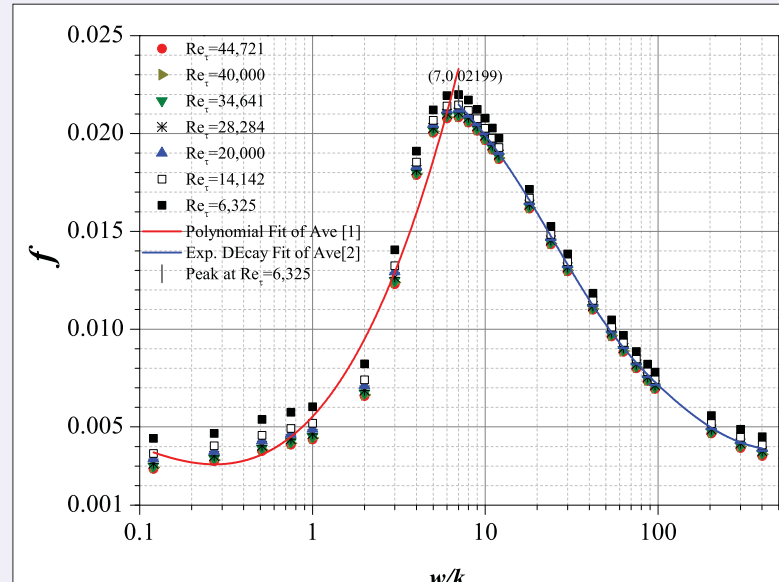


Figure 13: Scatter plot of the area-weighted average friction factor vs. w/k for a range of Reynolds numbers.

$$f = 0.005 + 0.01(w/k) + 0.01(w/k)^2 + 0.003(w/k)^3, \quad 0.12 \lesssim w/k \lesssim 7$$

$$f = 0.02e^{-(\frac{w/k}{41.03})} + 0.005, \quad w/k \gtrsim 7$$

Where: $f = \frac{(H/2)(-dp/dx)}{0.5\rho U^2}$

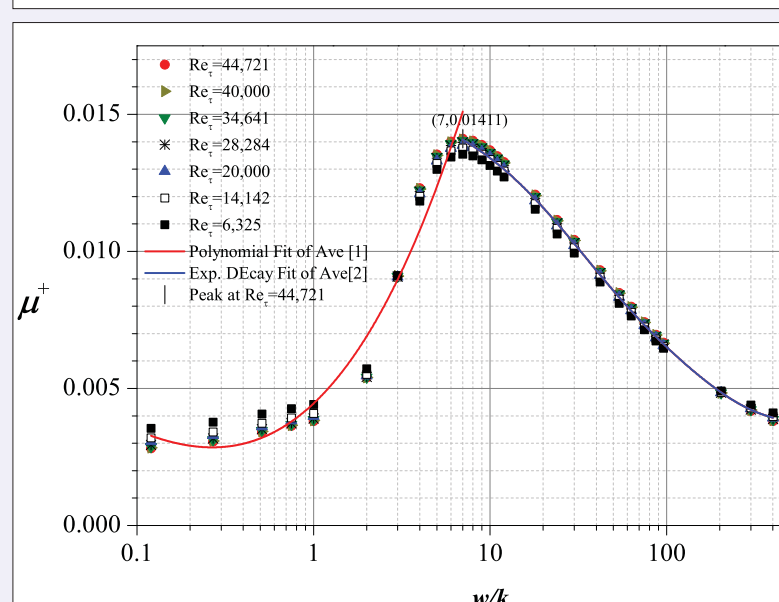


Figure 14: Scatter plot of the dimensionless eddy viscosity vs. w/k for a range of Reynolds numbers.

$$\mu^+ = 0.004 + 0.006(w/k) + 0.006(w/k)^2 + 0.001(w/k)^3, \quad 0.12 \lesssim w/k \lesssim 7$$

$$\mu^+ = 0.01e^{-(\frac{w/k}{56.13})} + 0.004, \quad w/k \gtrsim 7$$

Where: $\mu^+ = \frac{\mu}{\rho U (H/2)}$

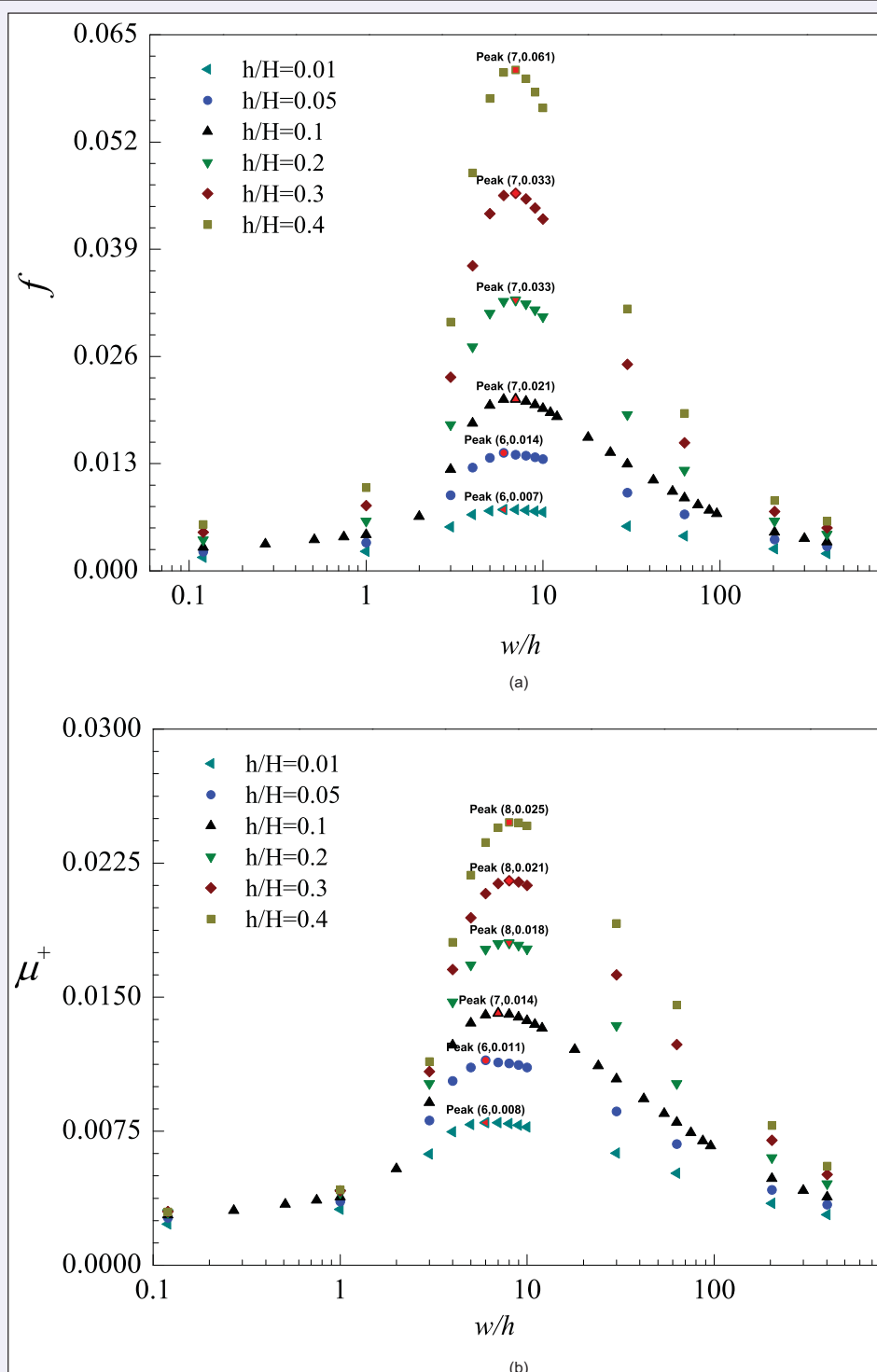


Figure 15: The effect of varying the roughness element height on (a) friction factor (b) the non-dimensionalised eddy viscosity.

Discussion and conclusions

The current results confirm that the optimum spacing of roughness elements to maximise friction and eddy viscosity within the flow occurs at $w/k=7$. It is found that this value is only weakly dependent on Reynolds number, and the decay rate of mixing and flow resistance as a function of w/k ratio beyond this optimum spacing is slow.

Figure 13-14 show respectively a linear rate of flow resistance and turbulent mixing up to $w/k=7$, followed by an exponential rate of perturbation decay beyond this critical ratio, with no significant dependence on flow Reynolds number.

The present results are pertinent to analyses of environmental flows over rough surfaces, here explored with reference to dilute, particulate, density-driven flows in deep marine setting (i.e., turbidity currents). Horizontal velocities within such flows tend to zero near the flow-ambient fluid interface and at the lower boundary, with an internal velocity maximum beneath which the flow can be well approximated as a shear layer.

Flow over erosional roughness may operate in addition to or instead of the commonly invoked hydraulic jump mechanism to cause enhanced turbulence and thereby sediment carrying capacity at locations such as submarine channel to lobe transitions.

Uncertainty over the relative magnitudes of these effects makes it unclear whether greater flow run-out will be promoted during flow over rugose substrates of width to height ratio $w/k \approx 7$; similar decay rates of drag and turbulent diffusion for $w/k > 7$ further suggest there may be no optimal higher w/k ratio over which a flow might experience maximal run-out; both these question await further work.

As illustrated in figure 15 (a)-(b), the varying h/H ratio has no significant effect on the optimal flow resistance and turbulent mixing.

Acknowledgments

This research was funded by the Turbidites Research Group industry consortium (Anadarko, BG, BHP Billiton, BP, ConocoPhillips, Maersk, Marathon, Nexen, Statoil, Tullow and Woodside.)

References

- Eggenhuisen, J.T., McCaffrey, W.D., 2012. The vertical turbulence structure of experimental turbidity currents encountering basal obstructions: implications for vertical suspended sediment distribution in nonequilibrium currents. *Sedimentology* 59, 1101–1120. doi:10.1111/j.1365-3091.2011.01297.x.
- Macdonald, H.A., Wynn, R.B., Huvne, V.A., Peakall, J., Masson, D.G., Weaver, P.P., McPhail, S.D., 2011. New insights into the morphology, fill, and remarkable longevity (> 0.2m.y.) of modern deep-water erosional scars along the northeast Atlantic margin. *Geosphere* 7, 845–867. doi:10.1130/GES00611.1.
- Meiburg, E., Kneller, B., 2010. Turbidity currents and their deposits. *Annual Review of Fluid Mechanics* 42, 135–156. doi:10.1146/annurev-fluid-121108-145618.
- Wynn, R.B., Kenyon, N.H., Masson, D.G., Stow, D.A.V., Weaver, P.P.E., 2002a. Characterization and recognition of deep-water channel-lobe transition zones. *Bulletin of the American Association of Petroleum Geologists* 86, 1441–1462.
- Engels, J.L., Edwards, M.H., Polyak, L., Johnson, P.D., 2007. Seafloor evidence for ice shelf flow across the Alaska-Beaufort margin of the Arctic Ocean. *Earth Surf. Proc. Land* 32, 1e17.